New Advanced Nanoporous Materials for Industrial Heating Applications

Arlon J. Hunt

Environmental Energy Technology Division

Lawrence Berkeley National Laboratory

Sponsored by the Department Of Energy

Industrial Technologies Program

Industrial Materials for the Future

Award Number: ED192453

Final Report

December 30, 2005

DOE Program Manager: Sara Dillich

Table of Contents

List of Figures

List of Tables

Project Overview

Objective

The goal of this project was to develop new advanced nanoporous insulating and refractory materials for industrial heating applications based on sol-gel processing, supercritical drying, and advanced processing techniques. Aerogel-based nanoporous ceramics are a new class of materials suitable for industrial heating applications. A new type of low cost nanoporous ceramic based on alumina, chromia, silica was successfully developed in this project. The small size of the pores and low solid content of these materials quenches the gas conduction and minimizes the solid conductivity of these materials. Long term sintering experiments indicate that this material is stable at a temperature 1050^{o}C for years. This material provides better insulation in high temperature furnaces and other industrial applications that will substantially reduce energy loss and enhance equipment life and operation.

Summary

Identified a material composition suitable for high temperature industrial insulation and refractory applications. The best composition was determined to be a specific formulation of Al_2O_3 and Cr_2O_3, with a small amount of silica as a stabilizer (referred to here as ACS).

Produced ACS gels using a variety of chemical pathways, initially using alkoxides of aluminum and chromium. Alcogels formulated using these starting compounds exhibited nanostructured properties after prolonged exposures to high temperatures.

Discovered a non-conventional route to the ACS gels allowing the use of inexpensive commodity chemicals instead of expensive alkoxide precursors. Calculations showed that the raw material costs dropped from $118 per pound to slightly over $2 per pound.

Fabricated blocks large enough for high temperature testing (15x15x1cm)

Our industrial partner, Applied Science Laboratories, Inc. performed conductivity measurements using the heat flow method at temperatures up to 1000ºC showing that the thermal performance is superior to existing products in the same price range.

Verified the long term stability of the material at high temperatures by conducting sintering tests at 1050ºC for over six months.

Accomplishments

Various nanostructured materials were evaluated for their suitability for use in the insulation panels and refractory blocks used by several industries in the IMF program. Physical characterization of the most promising candidates was performed. Particular attention was placed on materials that can be processed using currently available production methods, and, especially, could be prepared from low-cost raw materials. After an extensive survey of various materials, $Al_2O_3/Cr_2O_3/SiO_2$ (ACS) powder derived from a CO2-dried aerogel precursor met these criteria. This composition showed an excellent resistance to high temperatures, maintaining a surface area of 170 m2/g after heating at 1000°C.

The original preparations involved using alkoxide precursors. One of the most important technical barriers involved finding novel chemistry pathways that avoid the high costs associated with these alkoxide precursors. We have been successful in finding preparations that made use of commodity feedstocks, specifically, $Al(OH)_3$ and CrO_3 and a small amount of silica alkoxide. Once this preparation technique was discovered, it was scaled up from gram to kilogram quantities for thermal testing and evaluation. This proved to be a more difficult task than was anticipated.

We developed methods to produce larger blocks and performed thermal conductivity measurements on medium sized blocks of material in conjunction with our partner, Applied Science Laboratory. We conducted sintering tests on the materials to determine their long term stability and analytically investigated the effects of package design.

Technical Report

Background

Industrial process heat comprises 17% of the industrial energy consumption in the United States. Materials used for process heat technologies vary from conventional firebricks to highly specialized materials for particular environments. For many years the production of refractory materials for heat processing was a commodity business based on price-per-ton of refractory material. More recently, some domestic firms have begun to develop a higher margin specialty business where the purchasing decision is based upon the cost of refractory per ton of product produced. This places an increased emphasis on higher performance insulation to reduce the energy required for process heat. Engineered ceramic materials and composites offer higher performance in thinner packages thus increasing energy efficiency and capacity. The worldwide refractory market reflects to some extent the domestic situation. However, in general there is larger emphasis on traditional mine-and-mill techniques for refractory and insulating brick manufacturing. Some European led firms are investigating materials made using synthetic approaches.

There are several substantial economic benefits to the adoption of new composite materials in the thermal treatment industry. Improved strength composite materials will improve material lifetimes resulting in lowered replacement costs. Reduced impurities and careful choice of material composition will reduce impurities and unwanted compounds in melts and the need to remove them. In addition, the development of some types of synthetic silicates may reduce the melting and refining time in the production of glass. This development could significantly increase glass capacity without a major capital investment by the glassmaker. Since these improvements accrue to several heat processing industries the potential for economic benefits is considerable. There is also a role for high performance materials that have lower thermal mass so as to utilize less energy in rapid heating applications.

Sol-gel processing has only been used in a very limited way in the refractory producers and without the use of supercritical solvent extraction. Not using supercritical drying means that the material becomes a dense phase and cannot be used for producing composite materials via the CVI route. The refractory industry has not yet followed this relative new and developing process. We have used these techniques to develop a new class of insulating refractory materials that will improve the energy efficiency and performance in several of the Industries of the Future (IOFs). We have discovered new material processing routes to produce materials from commodity chemicals reducing the cost of the raw materials by nearly two orders of magnitude from converntional alkoxide precursors.

Low temperature insulating materials generally benefit from the low bulk densities obtainable with standard aerogel formulations. However, aerogel materials are not limited to such densities and can be prepared with porosities ranging from 25-99.9%.

At lower porosities, the mechanical weaknesses found in very high porosity aerogels are absent, though they still possess many of the desirable properties of low density aerogels, These include, an open pore network of mesopores and a tortuous solid network of nanometer-scaled solid particles. This results in a very low level of thermal solid conductivity even for higher density aerogels.

Approach

Several of the IOF's involve the processing of large quantities of material at very high temperatures, therefore requiring specialty thermal protection systems. Often, these are non-durable items which when past there usable lifetimes must be completely replaced. This results in considerable down-time, labor for replacement of insulations, and energy loss due to reheating loads. A highly engineered material such as an aerogel composite, provides exceptional thermal performance and, if designed properly, can meet or exceed the durability of current refractories. However, each IOF has operating requirements that are specific to the product being produced and therefore require a specific oxide/composite formulation. Examples of the types of aerogels targeted for specific IOF's are:

- Steel: SiO_2, Al/SiO_x, Al/MgO_x-Carbon, MgO, MgO-Carbon, Si/ZrO_x
- Aluminum: Cr/MgO_x
- Glass: MgO, Si/ZrO_x, Cr/MgO_x, SiO_2, Al/FeO_x
- Chemicals: Al/SiO_x, Al/FeO_x

The technical barriers include 1) finding a new high temperature material with desirable insulating characteristics, 2) reducing the high cost associated with starting materials based on gel forming alkoxide compounds, 3) minimizing the tendency of nanostructured materials to sinter at high temperatures resulting in an increase in solid conductivity, and 4) mitigating the increase in high thermal conductivities at high temperatures due to radiant heat transfer within the material.

The objective was to find a new high temperature insulating material composition with a stable nanostructure at high temperature with a porous nanostructure to reduce gas conduction. Aerogel-based composites provide many of the desirable characteristics required for a new class of materials for industrial heating applications. The small size of the pores in this material quenches the gas conduction, the low density minimizes the solid conductivity and the intrinsic optical properties aggregates block the radiant heat transfer. Once the desired material was produced with the optimized composition and pore size using available alkoxide routes, alternative processing methods were sought to reduce the cost of production. Alumina- and chromia-based materials with a high surface areas and open porosity are attractive materials for uses requiring a low thermal conductivity at high temperatures [1], or a stable microstructure for catalytic reactions [2, 3, 4, 5, 6 and 7]. Such nanostructured oxides can provide performance or efficiency improvements in both of these areas. In industrial heating applications, advanced porous materials would be expected to lower the thermal conductivity of refractory bricks or backing insulations, thereby significantly reducing energy consumption. While for

applications in catalysis, high surface areas and thermal stability give increased turnovers and yields in many cases. Synthesis and drying procedures leading to Al_2O_3 and Cr_2O_3 aerogels, as either primary or binary oxides, have been available for some time. Alumina aerogels are most commonly prepared by a standard sol–gel approach through the hydrolysis and condensation of a sterically hindered aluminum alkoxide, such as an s-butoxide, or an acetylacetonate [8, 9, 10 and 11]. However, there has been one recent report of the preparation of alumina aerogels by the reaction of aluminum nitrate with propylene oxide [12]. The use of alkoxide precursors is problematic due to their extreme cost and low ceramic yield. Chromia aerogels have been prepared by the reduction of CrO_3 by alcohols [13].

With the aim of developing a straightforward preparation of alumina–chromia aerogels from low-cost precursors, we describe the syntheses of such materials derived from $Al(OH)_3$ and CrO_3. These reagents react smoothly, by an acid–base process, to form a highly soluble salt which is available for further reduction by alcohols, yielding rigid gels. A further aim of this work was to determine the composition and processing conditions that lead to retention of a high surface area and porosity after exposure to high temperatures. In this regard, it has long been know that incorporation of a small percentage of SiO_2 into alumina aerogels greatly reduced their loss of surface area upon thermal exposure [14 and 15]. Therefore, we have concentrated our studies on ternary oxides of the $Al_2O_3/Cr_2O_3/SiO_2$ system [16]. The physical properties of these materials after conversion to aerogels by supercritical drying, and after subsequent treatment at high temperatures will be discussed.

Development of ACS Aerogels

Aerogels containing both Al_2O_3 and Cr_2O_3 were prepared by the reduction, by alcohols, of a precursor salt solution derived from $Al(OH)_3$ and CrO_3, followed by supercritical drying in either CO_2 or ethanol. TEM analyses showed a microstructure typical of aerogels, with a connected matrix of ~10-nm diameter particles and an open pore network. Subsequent thermal processing converts the initial aerogels to a high surface-area material comprised of Al_2O_3 and Cr_2C_3. Addition of ~6% SiO_2, relative to Al results in an increased retention of surface area at high temperatures. Surface areas of the aerogels after supercritical drying ranged from 240 to 700 m^2/g, while after treatment at 1000°C values ranged from 110 to 170 m^2/g. The composition which showed the greatest temperature stability was $2(0.94Al_2O_3 \cdot 0.06SiO_2)Cr_2O_3$. After treatment at 1000°C, all a samples contained a large number of crystallites of the Cr_2O_3 phase, eskolaite, with diameters ranging from 0.5 to 1.0 μm. An additional unidentified phase may also be present. The presence of these larger crystallites leads to a lower transmittance in the near-IR due to increased scattering, thereby reducing the radiative component of heat transfer and providing better insulation properties.

Experimental Procedures

$Al(OH)_3$, CrO_3 (99%), and tetramethoxysilane (TMOS) were purchased, and used as received, from Aldrich Chemical Corp. Freshly obtained quantities of the alkoxides tetraethoxysilane (TEOS, EM Science) Aluminum di(sec-butoxide)acetoacetic ester chelate (Alfa Aesar, Tech Grade) diethoxysilane-sec-butylaluminate coplymer (Gelest, Inc.) and polyethoxysilane (Silbond Corp., H-5 Grade) were used in all cases. Polyethyleneglycol (PEG-300) was obtained from Dow Chemical Corp. Methanol, ethanol, 2-propanol, and 1-butanol were obtained from various sources as anhydrous solvents and used without further purification.

Single-point BET surface area measurements were obtained using a Quantasorb surface analyzer (Quantachrome, Inc.) from the desorption of 30% N_2/He. Helium pycnometry and multi-point BJH pore size distributions were performed by the Micromeritics Materials Analysis Laboratory (Norcross, GA, USA.) A TA Instruments SDT 2960 TGA-DTA system was used for thermal analyses. X-ray diffraction powder patterns were collected on a Siemens Kristalloflex diffractometer using Cu Kα radiation. Samples for TEM analyses were ground, suspended in acetone, and evaporated onto holey carbon–Cu grids. TEM images were taken with a either a Topcon 002B microscope at 200 kV, or a JEOL 200CX analytical microscope with an ultrathin-window EDX attachment, operating at 200 kV. Near-IR transmission measurements were obtained with a Nicolet Magna-IR 760 spectrophotometer, using 3% (w/w) dispersions of the analyte in mineral oil.

Thermal treatment of dried aerogel samples was carried out in a box furnace under air, unless otherwise indicated. All samples were held at the desired temperature for 60 min.

Preparation of wet gels derived from aluminum hydroxide followed the following general procedure, using the reagent quantities listed in Table 1. The desired amounts of $Al(OH)_3$ and CrO_3 were placed in a tall-form beaker, to which a mixture of H_2O/17N HNO_3 was added. The exothermic reaction between the acidic CrO_3 and HNO_3 and basic $Al(OH)_3$ began instantly, and after 1–2 min of slow stirring the mixture existed as a bright orange suspension. At this point, samples were placed on a hot plate and gently heated for 20–30 min. During this stage, gas was released and the suspension changed to a deep red, highly viscous Al–Cr salt solution with no solids visible. This process was judged to be complete when the evolution of gas had ceased, but the solution was still thin enough to be stirred.

The stirring rate was then increased and the desired amount of alcohol was quickly added. If silica was desired in the final product, the silicon alkoxide precursor was dissolved in the alcohol prior to mixing with the Al–Cr salt solution. The reduction of the chromium IV present began immediately, forming a dark brown solution. Care was taken to ensure that all of the Al–Cr salt solution was dispersed before gelation, which, depending on the sol density, occurred in as fast as 30 s to over 3 h.

Table 1. Reagent ratios for aerogel syntheses and surface area results.

Sample	CR03 (mol)	$AL(OH)_3$ (mol)	NHO3 (mol) in 4ml H_2O	Alcohol:40ml	Si alkoxide	Notes	Surface area as dried M^2/gm	Surface area 450°C M^2/gm	Surface area 1000°C M^2/gm
A1	0.02	-	0.005	2-propanal	-	Very weak gel	290	13	13
A2	0.02	0.01	0.01	2-Propanal	-		270	180	41
A3	0.02	0.02	0.02	2-Propanal	-		260	160	44
A4	0.02	0.04	0.04	2-Propanal	-	Rigid gel	240	170	64
B1	0.02	0.04	0.04	2-Propanal	0.0024 TMOS	Brittle gel	350	-	130
B2	0.02	0.04	0.04	2-Propanal	0.0024 TEOS	Rigid gel	300	-	120
B3	0.02	0.04	0.04	2-Propanal	0.0024 polyethyl silicate	Brittle gel	530	-	110
C1	0.02	0.04	0.04	Methanol	0.0024 TEOS		360	-	120
C2	0.02	0.04	0.04	Ethanol	0.0024 TEOS		420	-	130
C3	0.02	0.04	0.04	2-Propanal	0.0024 TEOS		300	-	120
C4	0.02	0.04	0.04	1-Butanol	0.0024 TEOS	Soft gel	360	-	110
D1	0.02	0.04	0.04	Ethanol	0.0024 TEOS	PEG heat treatment after gelation	240	-	110
E1	0.02	0.04	0.04	Ethanol	0.0024 TEOS	Supercritical ethanol dried	700	-	170
F1	--	-	-	-	-	Alkoxide gel	350	-	130

The gels were then covered and placed in a sealed container under a saturated ethanol atmosphere to age for 24 h. The gels were often quite rigid, though their strength varied considerably in proportion to the original sol density. Most of the gels were dark brown in color; however, gels derived from very low density sols often appeared slightly green. After aging, the gels were removed from their containers and soaked in anhydrous ethanol in a bath of at least ten times the gel volume for 24 h. This soaking procedure was then repeated an additional two times. Though quite brittle, with great care the gels could often be removed from their containers as monolithic pieces. However, for convenience of handling and drying they were typically allowed to break into smaller pieces of about 1 cm^3 in size.

To evaluate the effect of high temperature prior to drying on the final aerogel's properties, one sample was soaked in 20 volumes of PEG-300 for 7 days. The sample

was then heated to 185°C for 180 min, during which time its color changed from brown to dark green. This sample was then exposed to a second set of three 24-h alcohol soaks to remove the PEG-300 before supercritical drying.

Drying of the wet gels, to produce the corresponding aerogels, followed standard CO_2 substitution and drying procedures [16,17]. The total process time was 18 h, and the process conditions were maintained at 5°C and 55 bar during the substitution phase, and 45°C and 90 bar during the drying phase. The aerogels generally appeared dark green-brown to black and were effectively opaque. Shrinkage of the gels during this stage was relatively slight, and the samples maintained ~60–70% of their original volume.

For comparison, one sample was dried using the supercritical ethanol method. A 25 ml piece of this sample along with an additional 20 ml of ethanol, was placed in a 200-ml vessel which was then pressurized to 67 bar with dry nitrogen. The vessel was heated to 300°C over a 45 min period, and the pressure was maintained at 67 bar by venting the contents when needed. The system was held at this temperature for 30 min and was then slowly vented to ambient pressure. The aerogels dried in this way were dark green, and exhibited slightly more shrinkage than their CO_2-dried counterparts, retaining only ~40–50% of their original volume.

An aerogel derived from alkoxide precursors and CrO_3 was also prepared for comparative purposes. This sample (F1) was prepared by mixing 30 g (29.1 ml, 0.1 mol) Aluminum di(sec-butoxide)acetoacetic ester chelate, 2.25 g (~2.2 ml, ~0.006 mol Al/0.0056 mol Si) diethoxysilane-sec-butylaluminate coplymer, and 220 ml of ethanol to which 5.0 g (0.05 mol) CrOs dissolved in 30 ml of water was added with vigorous stirring. The mixture formed a rigid brown gel within 1–2 min. The gels were then aged for 24 h, followed by a soaking procedure as described above, and dried using the CO_2 method.

Chemical and Physical Properties of ACS

The specific surface areas of the various gels studied here are summarized in Table 1. Several sets of gel recipes were evaluated to determine the composition which maintained the highest surface area after exposure to high temperatures. Series A evaluated the effect of the Al/Cr ratio, which produced a considerable variation in the final surface areas. The unbaked aerogels gave the highest surface area when Al/Cr was low, though the values were fairly similar. After heating to 450°C, the temperature at which most of the mass loss has already occurred, a this trend is continued, with the notable exception of the aluminum-free sample Al that has lost the majority of its surface area. However, after heating to 1000°C, the trend reverses, and the samples with the highest Al/Cr ratios the most surface area.

The effect of the addition of 6% (mol/mol) silica, relative to alumina, from various silicon alkoxide precursors if shown in series B. In all cases the addition of silica results in a significant increase in the surface area of the freshly dried aerogel, and a large increase, of around 2×, in the surface area after baking at 1000°C.

Series C shows the effect of the type of alcohol used as solvent and reductant for the gelation. The variation is not large; however ethanol gives the highest value for both the original aerogel (420 m^2/g) and for the sample after baking at 1000°C (130 m^2/g).

Additionally, three special cases were also measured. A gel prepared by the recipe of sample C2, but heated to 185°C in PEG-300 (sample D1), possessed a relatively low surface area in both the original aerogel (240 m^2/g), and the aerogel baked at 1000°C (110 m^2/g). Sample E1, with the same composition as C2, but dried using supercritical ethanol, gave the highest surface areas of any aerogel measured, 700 m^2/g for the original aerogel, and 170 m^2/g after baking at 1000°C. Finally, the alkoxide-derived aerogel gave surface area results comparable to those of the samples from series C.

The effect of high temperatures on the alumina–chromia aerogels is revealed by the TGA plots shown in Fig. 1. Both the aerogel derived from $Al(OH)_3$, sample C2, and the alkoxide-derived gel, F1, show most of their mass loss at relatively low temperatures with the majority occurring below 400°C. Sample C2 retains approximately 47% of its mass after heating to 1000°C, while sample F1 shows a somewhat higher mass retention of 55%.

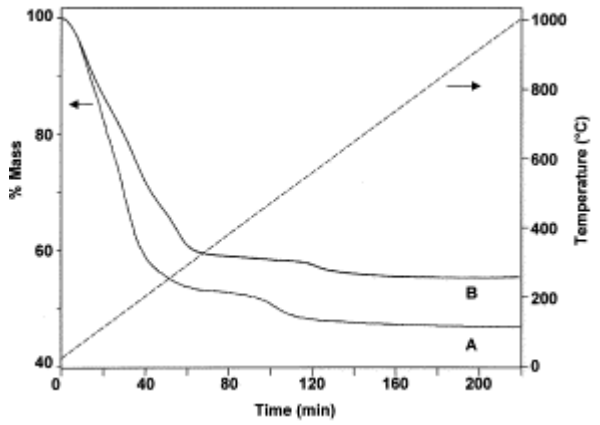

Figure 1. TGA plots of (A) alumina–chromia aerogel derived from $Al(OH)_3$ (sample C2), and (B) from aluminum alkoxides (sample F1).

The skeletal densities of sample C2 before and after thermal treatments were determined by helium pycnometry. The original aerogel, gave a value of 1.92 g/cm^3, while the same sample baked at 450°C had increased to 2.69 g/cm^3 and the sample taken to 1000°C to 3.59 g/cm^3. The value for the thermally treated sample is somewhat less than might be expected for a mixture of alumina (3.9 g/cm^3) and chromia (5.2 g/cm^3), suggesting the presence of closed porosity.

Figure 2 gives examples of TEM images of sample C2. In the top image, of the original aerogel, a structure common to many aerogel material is observed. Irregularly shaped primary particles with dimension on the scale of 10–20 nm, are linked in an extended network surrounding regions of open porosity. After baking at 1000°C, a considerable change in structure is evident as seen in the bottom image. The porous network of small

particles is still present, but a considerable coarsening of the particle size and closure of much of the porosity is evident. More significant, however, is the presence of large crystallites within the aerogel network. These appear fairly evenly distributed throughout the sample and were consistently observed in many micrographs. The images suggest two morphologies, however, this can not be determined conclusively. Circular, or oblong, shapes with diameters approaching 1 μm are common. Smaller, rod-shaped object are also readily seen, with lengths on the order of 0.5 μm. It is possible, however, that there is only one morphology, approximating platelets, and the objects that appears as rods are actually these platelets viewed edge-on.

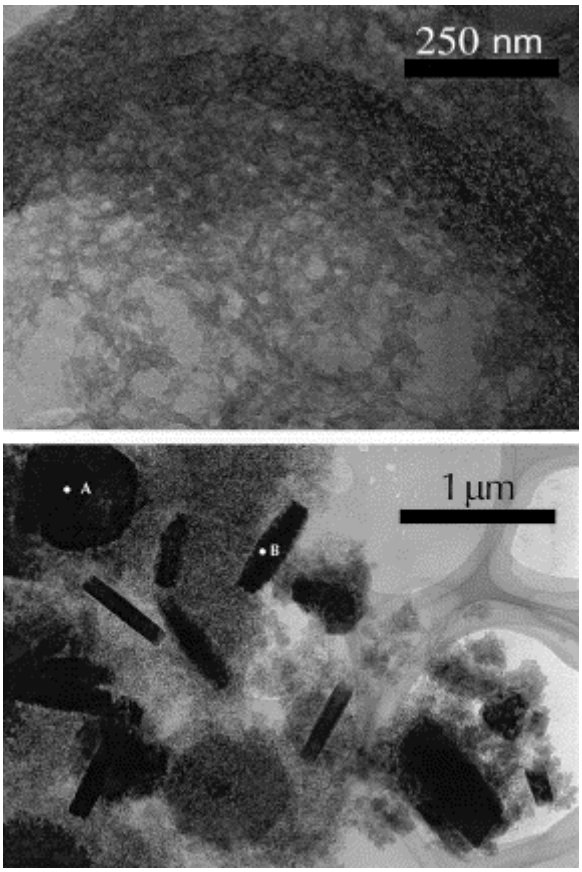

Figure 2. TEM micrographs of sample C2. Top: original aerogel without thermal treatment. Bottom: Same sample after baking at 1000°C.

Pore size distribution curves derived from nitrogen desorption isotherms appear in Fig. 3(a)–(c). Aerogels of sample C2 without thermal treatment and after baking at 450°C and 1000°C are shown in Fig. 3(a). The peak of the pore volume curves is at 20–30 nm in all three cases, however, a steady loss of pores with diameters <10 nm is seen as the baking temperature is increased. This effect is seen more drastically in Fig. 3(b), which shows the pore distribution for sample E1, the sample dried using the supercritical ethanol method. In this case the unbaked aerogel contains a much higher fraction of pores with diameters <10 nm, though the peak of the distribution is again in the range of 20–40 nm. After heating at 1000°C, most of the small pores have been lost, as well as a considerable

fraction of the overall porosity. The peak of the distribution remains at ~25 nm, however. Finally, Fig. 3(c) gives the pore distribution curves for aerogel sample D1, the sample that was heated in PEG prior to supercritical drying. An overall lower porosity is observed in both the unbaked aerogel and the aerogel after baking at 1000°C, relative to the previous samples. The peak distribution for the unbaked aerogel again falls between 20 and 50 nm, and a significant amount of <10 nm pores is also seen. After baking the peak of the distribution curve has shifted slightly, to ~30 nm, and the small pores have once again been lost.

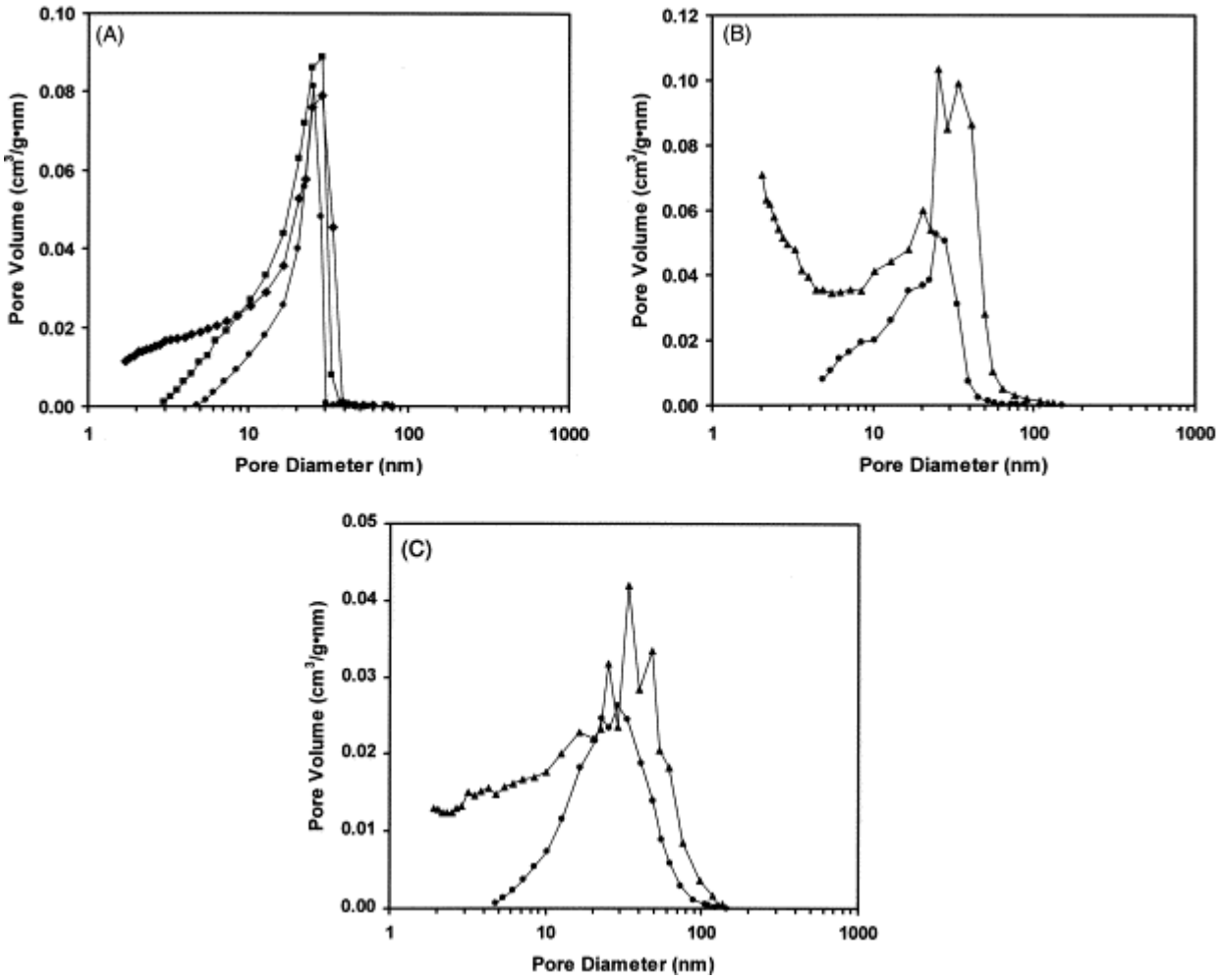

Figure 3. Pore size distribution plots of aerogel samples. (a) Sample C2: (♦) original aerogel, (▪) after baking at 450°C and (•) after baking at 1000°C; (b) sample D1: (♦) original aerogel and (•) after baking at 1000°C; (c) sample E1: (♦) original aerogel and (•) after baking at 1000°C.

The distribution of chemical species within the aerogel samples was evaluated using EDX spectroscopy. Sample C2 was investigated both as the original aerogel, and after baking at 1000°C. The unbaked aerogel, examined at many points, showed a fairly consistent distribution of Al and Cr throughout the sample. The number of counts for the

Al peak is typically 1.5 times that of the main Cr peak. In the case of the heat treated sample, however, the TEM results suggested a considerable inhomogeneity. In regions where the sample consists of a microporous aerogel-like structure, the ratio of Al to Cr is much higher, with the number of counts for Al typically four times that of Cr. For the larger crystallites, the EDX spectra are shown in Fig. 4. The top spectra in Fig. 4 corresponds to point A in Fig. 2, a point taken over one of the larger irregularly shaped crystallites. In this case the Cr peak dominates the spectrum, showing almost five times the counts as the Al peak. However, the rod-shaped crystallites show the reverse case, with the Al peak giving ~2 times the counts as the Cr peak, as seen in the bottom spectrum of Fig. 4. This shows that a significant amount of phase segregation occurs as the aerogel is exposed to high temperatures, with Cr migrating out of the microstructured aerogel-like areas of the sample and into the newly formed large particles. These spectra also suggest that the two particle morphologies observed by TEM may indeed represent different chemical species. However, the effect of the aerogel-like material, which may entirely surround the crystallites, may introduce uncertainty into these measurements.

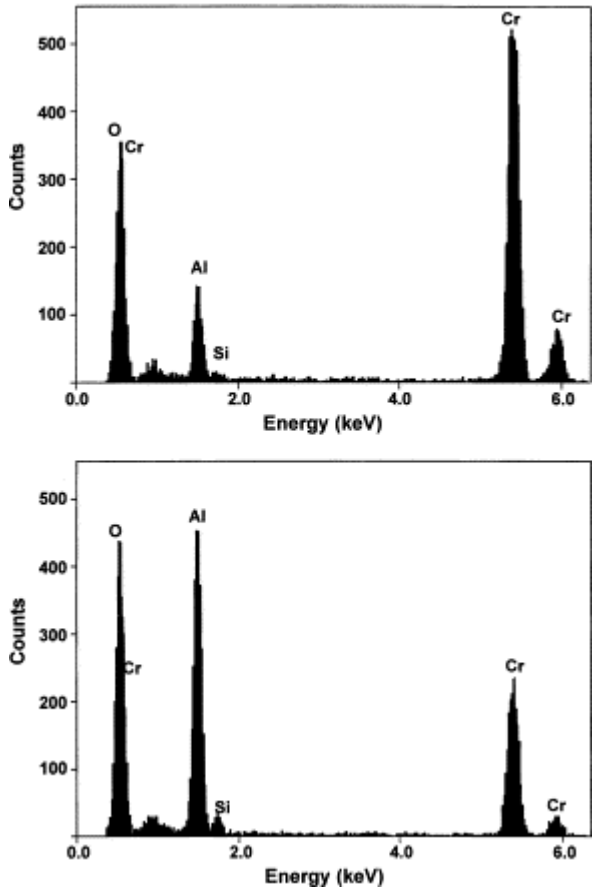

Figure 4. EDX spectra of sample C2 after baking at 1000°C. Top: point in Fig. 2 marked by A; bottom: point in Fig. 2 marked by B.

To better elucidate the nature of the crystalline species present after treatment at 1000°C, XRD patterns were obtained, and these appear in Fig. 5. Patterns for sample C2, D1, and

F1 all show one major phase, the Cr_2O_3 phase, eskolaite. Sample C2 does not exhibit any additional peaks or features other than those for eskolaite. The sample heated in PEG, D1, does not show additional strong peaks, but does possess a broad feature at low angles ($20<2\theta<40$) with a greater intensity relative to sample C2. This feature is commonly seen in the XRD patterns of amorphous aerogel materials. The pattern for sample F1, the alkoxide-derived aerogel, shows additional peaks at $2\theta=30°$, 35° and 63°. These peaks exhibit some similarities to the SiO_2 phase, shistovite; however the match is not exact. The pattern for the ethanol-dried sample E1, was virtually identical to that of its CO_2-dried counterpart, sample C2. Sample C2 does not show any patterns which could be attributed to a second, aluminum-rich, crystalline phase as suggested by the EDX analysis. However, literature patterns for $Al_{1.4}Si_{0.3}O_{2.7}$, a phase with a similar Al to Si ratio to that of sample C2, shows only two XRD peaks, at $2\theta=24.5°$ and 66°. Since these peaks would potentially be covered by two eskolatite peaks at approximately the same position, the existence of this phase can not be ruled out.

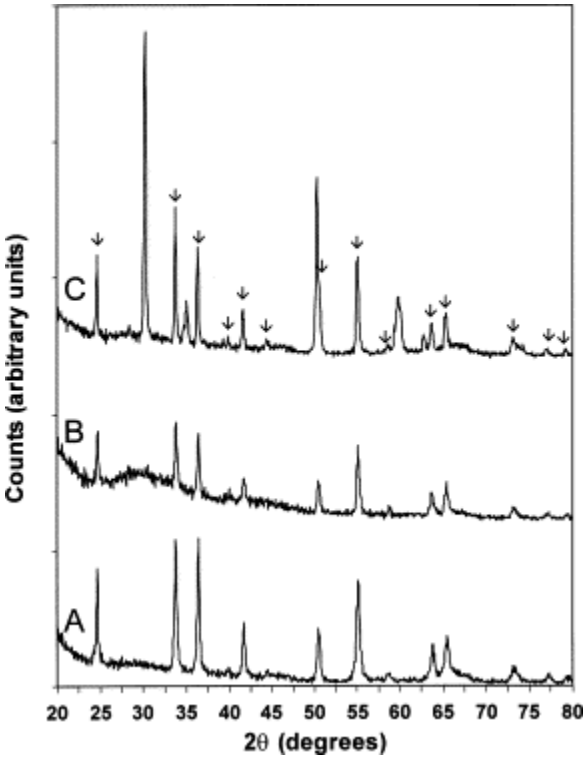

Figure 5. XRD patterns for aerogels after baking at 1000°C. A: sample C2, B: sample F1, C: sample D1. Arrows above plot **C** correspond to literature patterns for the Cr_2O_3 phase, eskolaite.

The presence of larger crystallites in the aerogels after exposure to high temperatures suggests that these materials may show a lower transparency in the near infrared, due to increased scattering by these inhomogeneities. The near-IR spectra of samples C2 and F1 appear in Fig. 6. Sample C2, with a higher proportion of larger crystallites, as determined by TEM, shows a more significant decrease of transmittance at shorter wavelengths, relative to sample F1. The absolute transmittance of sample C2 is lower and the slope of the spectrum is greater in the region from 8000 to 5000 cm^{-1}. This indicates a decrease in transparency at these frequencies, corresponding to the higher number of large crystallites in this sample. This of course implies a lower thermal conductivity a high temperatures [18].

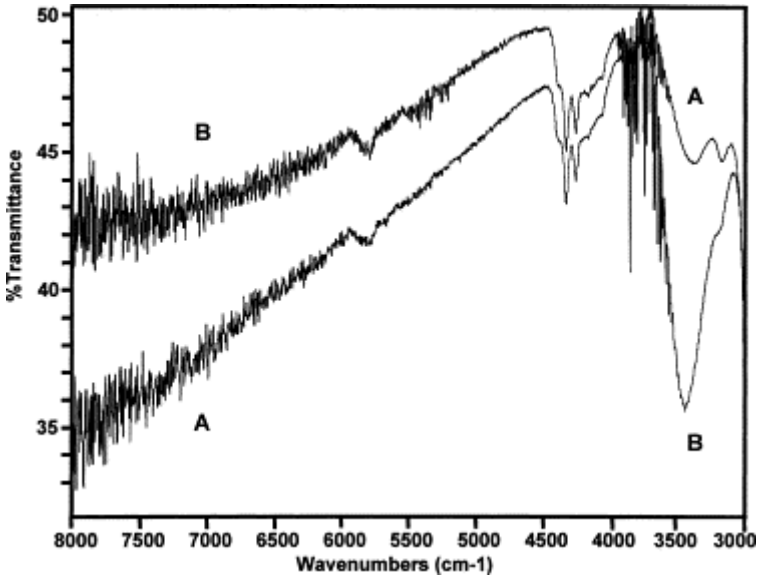

Figure 6. Near-IR spectra for aerogels after baking at 1000°C. A: sample C2 and B: sample F1.

Thermal Properties of ACS

After fabricating a large panel for thermal characterization, it was sent to Applied Science Laboratories in southern California for high temperature thermal conductivity measurements. Measurements of this type are very difficult to perform. Only a few laboratories in the world are capable of this type of high temperature measurement. Several attempts were made by other organizations to provide this data using the laser photolysis method. This involves heating the sample to a high temperature, then flashing one surface of the sample with a high powered pulse laser and watching the time dependence of the temperature rise on the back face. This is a relatively insensitive method and to obtain good results for a highly insulating material like aerogel the samples must be made unrealistically thin (< .3 mm).

We had developed a thermal conductivity apparatus at LBNL earlier [19] but it was not capable of the high temperatures required for the ACS testing. We were fortunate to find a partner to collaborate with on the conductivity testing. Applied Science Laboratories has developed a heat meter apparatus that directly measures the thermal conductivity at high temperatures by steady state heat flow. Table 2 gives the specifications for the ASL heat meter. Figures 8 and 9 show a diagram and picture of the apparatus respectively. ALS carried out an extensive testing program on a large sample (15 x15 cm) that we had fabricated as described earlier.

Figures 10 -12 summarize the results of the thermal conductivity measurements. Figure 10 gives the thermal conductivity as a function of temperature for one atmosphere pressure and under vacuum. The results of the thermal conductivity testing under one atmosphere of nitrogen indicated that the thermal conductivity was quite low with a small positive temperature dependence given by $k(T) = .046 + 7.14 \times 10^{-5} T$ (W/M^oK). The thermal conductivity results in a vacuum were about a three times lower with similar temperature dependence. Considering that the space shuttle tile was the result of multibillion dollar effort, and the cost of the tile is measured in hundreds of dollars per board foot, this was an encouraging result as the projected cost of the aerogel is only several dollars per board foot.

Figure 11 provides a comparison of the thermal conductivity with space shuttle tile as a function of temperature for ambient and vacuum pressures. I can be seen that the ACS outperforms the space shuttle tile at higher temperatures under ambient conditions. Figure 12 compares the thermal conductivity with various densities of firebrick. It illustrates the ACS has about one half the thermal conductivity of the lowest density firebrick tested and is considerably better than all the other higher density firebricks. The measurement is time consuming; (2 – 3 days per data point) the instrument provides reliable data with ±10% uncertainty in measured thermal conductivity.

The pressure dependence of the aerogel thermal conductivity indicates that, while attenuated, the gas component of the thermal conductivity could be decreased further by lowering the mean pore size of the aerogel material. Further improvement can be achieved by the addition of fibers or particles to further absorb and scatter the radiant component of thermal conductivity.

Table 2. Applied Sciences Laboratory heat meter specifications.

Temperature Range	300 to 1300K
Thermal Conductivity	k: 0.005 to 1 W/m-K, ±10% uncertainty
Specimen size	15x15x2.5cm

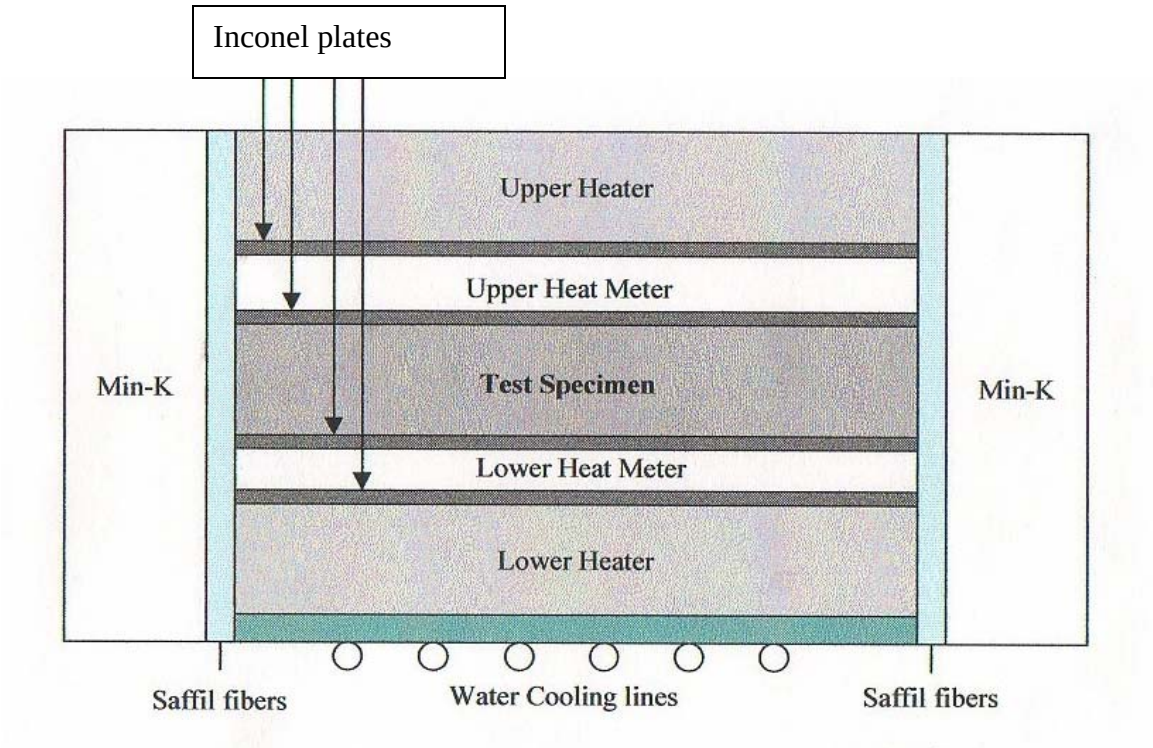

Figure 8. Diagram of the Applied Sciences Laboratory heat meter apparatus.

Figure 9. Photo of Applied Sciences Laboratory heat meter.

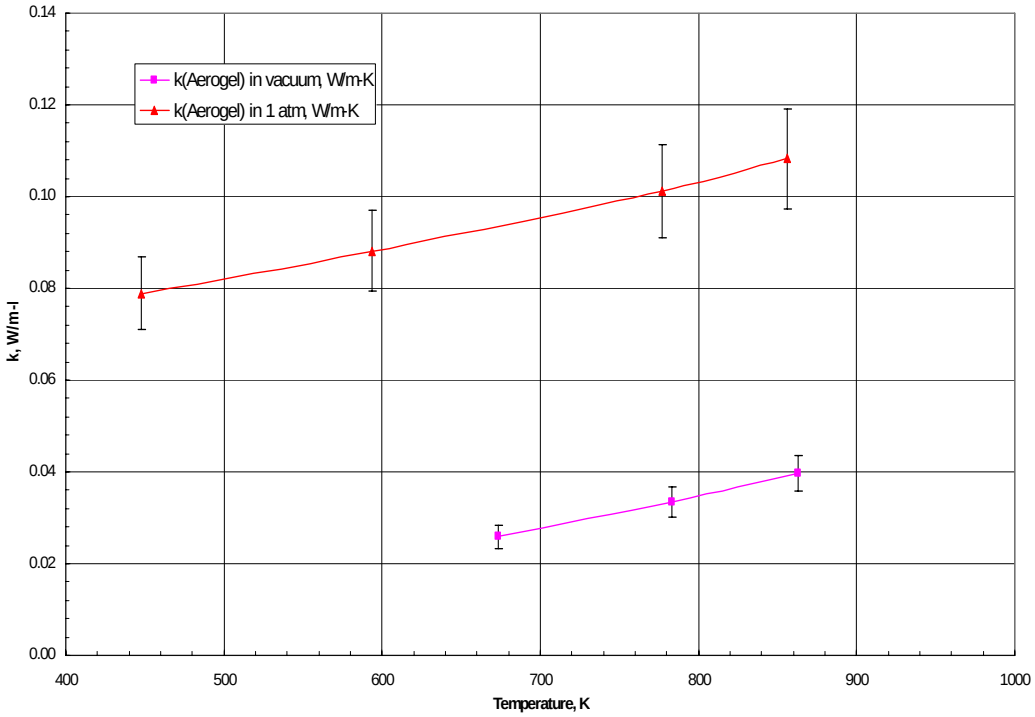

Figure 10. Applied Sciences Laboratory measurements of the thermal conductivity of ACS.

Aerogel, Vacuum

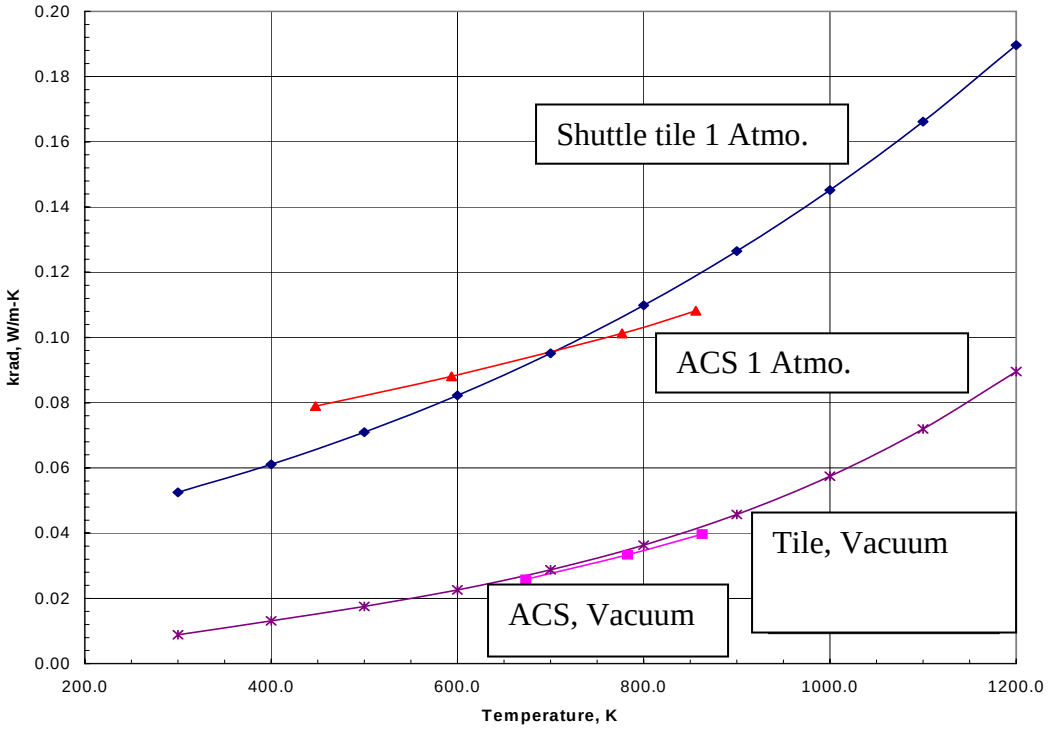

Figure 11. Comparison of ALS with shuttle tile thermal conductivity.

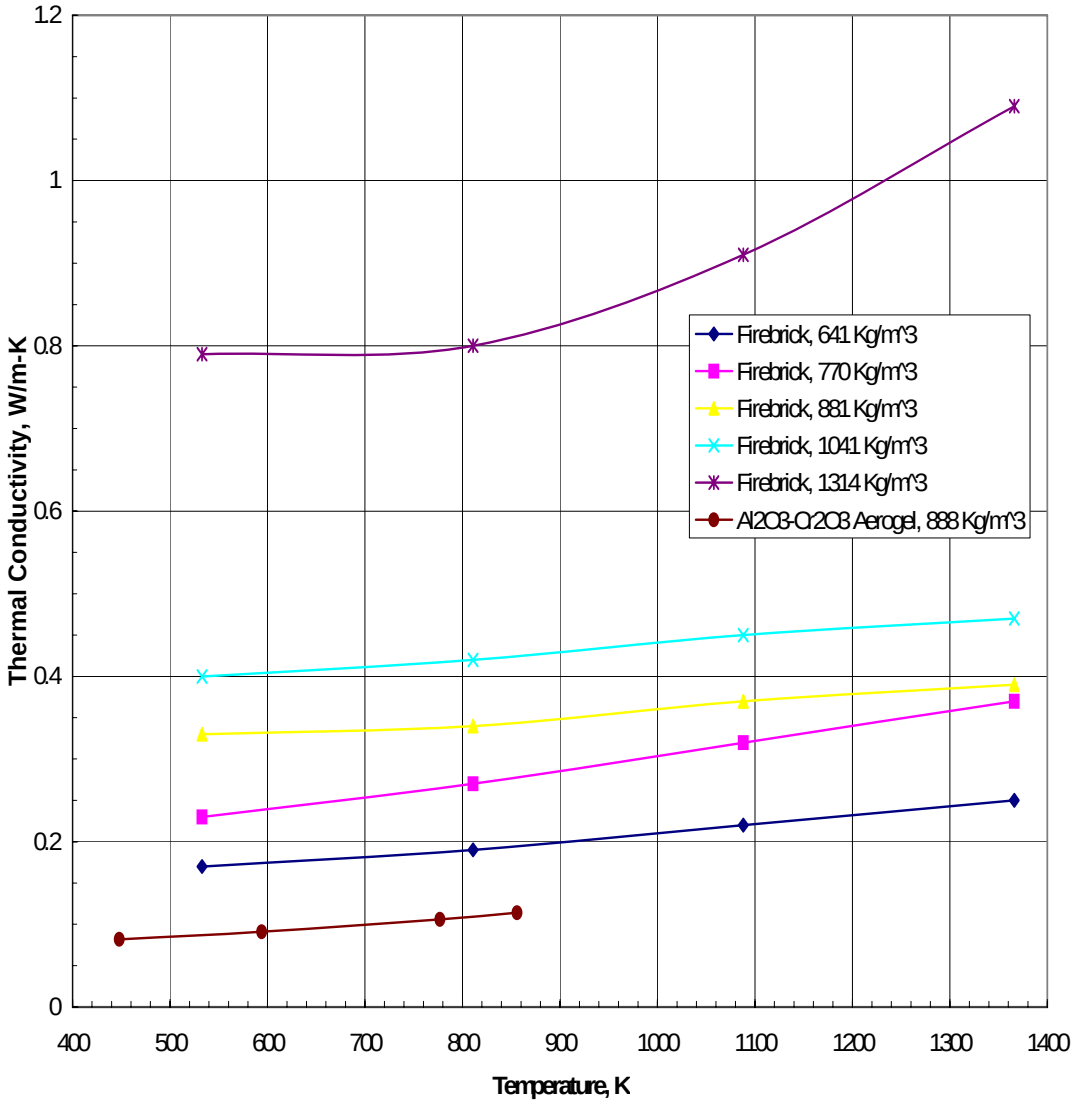

Figure 12. Comparison of thermal conductivity with competitive materials

We carried out thermal testing to define the long term sintering characteristics of ACS. We performed a series of studies at 1000°C and 1050°C to quantify the sintering behavior. The long term stability of the material is of utmost concern for its use in industrial heat applications. The results of the sintering tests are given in Fig. 13. The studies show less than 3% shrinkage over nearly 2000 hours at 1000°C. We accelerated the tests at 3000 hours by increasing the temperature to 1050°C and the sample shrank by only 4% by the end of testing after 6300 hours. This indicates good long term stability of the material at high temperatures.

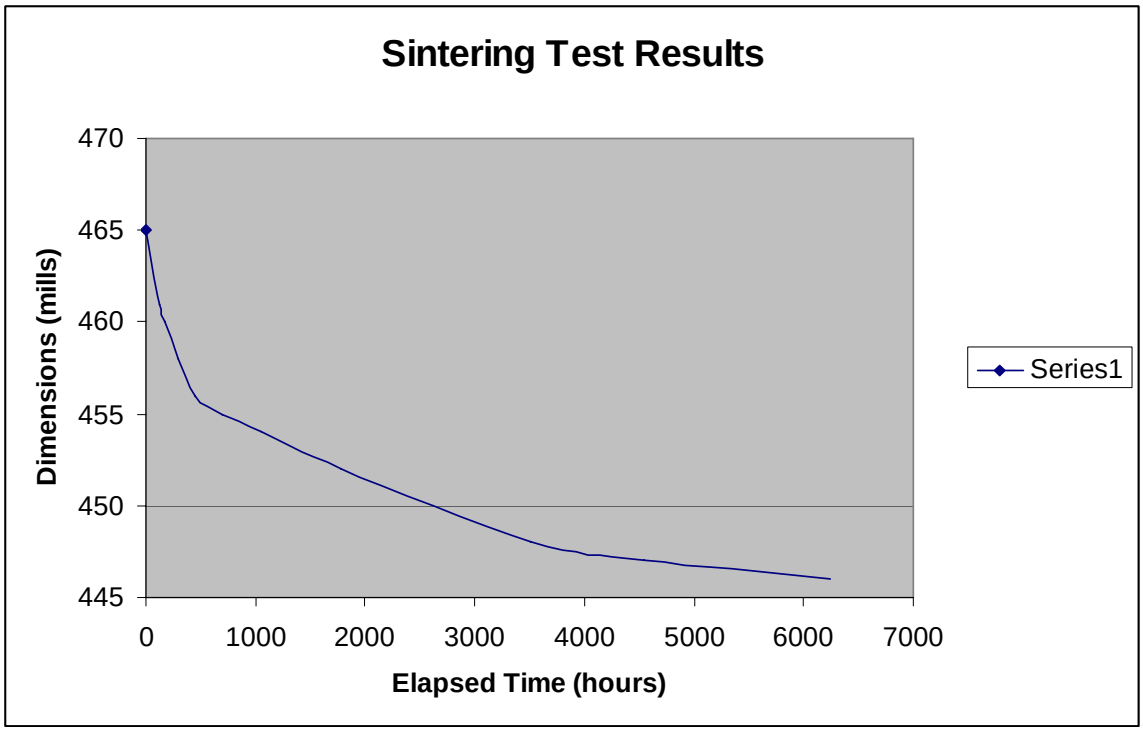

Figure 13. Results of sintering tests of ACS at 1050°C.

Discussion

The reaction between $Al(OH)_3$ and CrO_3 provides a convenient precursor to aerogels containing both Al_2O_3 and Cr_2O_3. The ratios of these oxides can be varied over a fairly wide range without drastically affecting the ability of the precursor solution to form a rigid gel. However, it was found that the addition of one equivalent of HNO_3, relative to $Al(OH)_3$ yields gels with greatly improved homogeneity and stiffness. The critical aspect to the syntheses of good-quality gels is allowing the initial reaction of $Al(OH)_3$ and CrO_3 to go to completion before attempting the reduction with alcohol. If the reduction is attempted too early, such as when solids are still present in the mixture, the sol will not gel but will form precipitates. Timing this step of the synthesis properly is, therefore, quite important. As mentioned above, the evolution of gas should have ceased before reduction, but the mixture should still possess a viscosity that allows it to be stirred. The nature of the gas evolved in this step was not determined in this study; however it is likely O_2 released by the conversion of CrO_4^{2-} to $Cr_2O_7^{2-}$.

The reduction step proceeds smoothly if the salt solution precursor has been prepared properly. Various alcohols can be used for this step, and it is likely that many other species can serve as both solvent and reductant as well. The solids content of the wet gel can be varied somewhat by adjusting the amount of alcohol used. Relative to sample C2, rigid gels could be prepared with twice the solids content by using half as much alcohol. Preparing very low solids content gels was somewhat more limited in scope. The practical lower limit for solids content, below which the sols would not gel, was

approximately 45% that of sample C2, and was achieved by increasing the volume of alcohol used by the corresponding amount.

Drying the wet gels to produce the corresponding aerogels is straightforward using either the low-temperature CO_2 substitution method, or the high temperature supercritical ethanol method. When CO_2 drying is used, there is a very modest amount of shrinkage to 50–70% of the original volume, and the gels appear dark brown to black. The absolute amount of shrinkage is difficult to determine, due to the irregular shapes of the aerogel pieces. When ethanol drying is used, the shrinkage is higher, to perhaps 30–50% of the original volume, and the aerogel is now dark green in color. This indicates that the conversion of CrO_2, the initial product of the reduction of Cr^{VI}, to Cr_2O_3 has begun during the drying stage. This was also observed in sample D1, during its pre-drying heat treatment in PEG-300.

Thermally treating the aerogels produced in this way leads to loss of around 50% of the original mass of the sample. This results from the loss of several volatile species evolved as the aerogel is heated. The chemical nature of the species presumed to be present at various stages of this process is as follows. The precursor salt solution, for the composition used in sample C2 and omitting the small fraction of silica present for clarity, is comprised of $2[Al(OH)^{2+}] \bullet [CrO_4 \bullet 2(NO_3)]^{4-}$, or a similar formula containing dichromate ions. After reduction by alcohol, the gels likely consist of, $2[Al(OH)(NO_3)]O \bullet CrO_2$. High temperature treatment of this material, would release water from the condensation of –OH groups, NO_2 from the pyrolysis of $–NO_3$ groups, and O_2 from the conversion of CrO_2 to Cr_2O_3. This would account for a mass loss of only 27%. The higher observed mass loss of 55% may then result from the loss of free water or alcohol trapped in the aerogel matrix, or possibly from the loss of $–CO_3$ groups that could be formed during CO_2 drying.

The desirable physical properties for a material of this type when used in high temperature applications, would be a stable microstructure with a high surface area, and an open pore network of with a high total pore volume. With regards to maintaining a high surface area the composition of sample C2 produces the best results. The addition of approximately 6% silica, relative to alumina, and use of a high Al/Cr ratio are the key factors in maintaining the surface area of the aerogel when exposed to high temperatures. The use of TMOS as the silica source, as in sample C1, does lead to a higher surface area, but the effect is not large, and does not outweigh the cost and safety advantages of using TEOS.

The production of aerogels that maintain a very low density after thermal treatments proved to be more problematic. Gels with lower solids content could be synthesized. However, due to the generally weaker solid network in these cases, the gels exhibited slightly more shrinkage during supercritical drying, and much more after exposure to high temperatures. This gives the result that aerogels produced from gels with low solids content and those prepared from gels with higher solids contents lead to aerogels with similar bulk densities after thermal treatment. The observed bulk volume of the aerogels after heating to 1000°C was generally no more than 10–15% of the volume of the original

wet gel. Heating the aerogels under alternate atmospheres, such as argon, 100% O_2, or vacuum did not significantly, or reproducibly, affect the loss of porosity and shrinkage of the aerogels.

The pore size analyses of the aerogels produced here do not provide a complete understanding of the changes to their pore structures upon heating the samples. A distinctive feature of the changes seen in the aerogels is the loss of small pores with diameters <10 nm. This was seen in all cases, most notably in the sample dried using supercritical ethanol (E1). In that sample a very high number of small pores were present initially. This may have resulted from the initial protection of this porosity by the formation of –OEt groups via esterification reactions during drying. This effect is known to occur during the alcohol drying of silica aerogels and can restrict pore collapse by blocking surface condensation reactions. However, if this occurred in sample E1, its subsequent exposure to high temperatures would lead to removal of these –OEt groups and loss of porosity.

The loss of small pores can not account for the entire loss of bulk volume observed upon heating the aerogels. The total pore volume for sample C2 after heating to 1000°C was still 66% of that of the original aerogel, as measured by Na adsorption. Additionally, the peak of the pore size distribution curve remains largely unchanged, near 25 nm. This suggests that the high shrinkage seen in these aerogels results from the loss of very large pores, with sizes not detected by gas adsorption methods.

The surface areas for these aerogels are typically maintained in the range of 100–150 m^2/g after heating to 1000°C for 60 min. This is similar to alumina–silica aerogels prepared by other methods. However, the presence of larger crystallites with dimensions on the order of 0.5–1.0 μm must lead to a lower average surface area. Therefore, the actual surface area of the finer-structured portion of these aerogels, consisting of alumina-rich nanoparticles, must be considerably higher.

The formation of large crystallites of eskolaite, Cr_2O_3, provides insight into the structure of the original gel formed upon reduction of the precursor salt solution. Al_2O_3 and Cr_2O_3 show a high mutual solubility and the fact that large crystallites of Cr_2O_3 form at high temperatures reveals significant phase segregation must be present in the original wet gel. It is, therefore, likely that the gelation of CrO_2, being the daughter species of the primary reaction of chromate with alcohol, occurs first. This is followed by precipitation and gelation of the aluminum salt, which is no longer soluble after the removal of the chromate, or dichromate, counter ion. TEM images of the original aerogel do not show a large distribution of particle sizes, so if the gelation does occur in two steps, the scale of the two networks must be similar. The network of CrO_2 particles can then coalesce into larger particles upon heating. This is demonstrated by sample A1, which does not contain aluminum, and shows a decrease in surface area from 290 to 13 m^2/g after heating to 1000°C.

The formation of larger crystallites may, however, provide advantages if these aerogels are to be used in high temperature insulation applications. The transmission of thermal

energy though radiation greatly outweighs the contribution of solid and gaseous conductivity at high temperatures. Therefore, radiation must be blocked by adsorption, scattering, or reflection for an insulation to be effective at these conditions. The oxides Al_2O_3 and Cr_2O_3 are reasonably transparent in the IR, especially at shorter wavelengths, which are dominant in the blackbody emission at temperatures of 1000°C and above. Because of this, insulations based on these, or other, nanoporous oxides typically include an additional phase with larger dimensions to enhance the scattering of the transmitted light and increase their opacity. In the case of the aerogels produced here, a larger-scaled feature is already present within the nanoporous network. This results in these materials showing a significant degree of self-opacification in the near-IR. This can be seen in Fig. 6, where the thermally treated aerogel derived from sample C2, with a large number of included crystallites, shows a lower transmittance compared to sample F1, derived from alkoxide precursors, with a lower number of crystallites. Further modifications to the synthesis and drying procedures to produce aerogels which retain a very low density after heat treatment could yield materials with an exceptionally low thermal conductivity at high temperatures.

Conclusions

Aerogels containing both Al_2O_3 and Cr_2O_3 may be conveniently prepared by the reduction, by alcohols, of a precursor salt solution derived from $Al(OH)_3$ and CrO_3, followed by supercritical drying in either CO_2 or ethanol. Subsequent thermal processing converts the initial aerogel to a highly porous, high surface-area material comprised of Al_2O_3 and Cr_2O_3. The composition that retains the finest nanostructure after thermal treatment contains an Al/Cr ratio of 2:1, with an addition of ~6% SiO_2, relative to Al. Thermal treatment at high temperature leads to the crystallization of a portion of the solid network into particles with diameters of 0.5–1.0 μm, with only one phase being positively identified as eskolaite, Cr_2O_3. Relative to supercritical drying in CO_2, drying in supercritical ethanol leads to a somewhat higher surface area, but does not reduce the total shrinkage combined from the drying and thermal post-treatment steps. Similarly, performing a thermal aging step in a high-boiling point solvent prior to supercritical CO_2 drying gives a slightly lower surface area but also does not reduce the total shrinkage of the aerogel during drying and thermal processing. The samples prepared using various reagent ratios and conditions consistently retained about 15–20% of the volume of the original wet gel after both supercritical drying and baking at 1000°C.

However, the retention of a high surface area and a significant fraction of the original porosity after exposure to high temperatures may allow these aerogel products to find uses as components of high temperature insulations, refractories, or catalysts. Use of these aerogel-derived materials in such applications will be greatly aided by the low costs of the raw materials used in this process. Both $Al(OH)_3$ and CrO_3 are commodity chemicals, with costs orders of magnitude lower than the alkoxide-based precursors commonly used to synthesize aerogels by conventional sol–gel processes.

The thermal characterization of the ACS material confirmed that it has a very low thermal conductivity at high temperatures with a small positive increase with temperatures. It outperforms existing firebrick and is the equal or better that space shuttle tile (although the higher atomic number of the constituents means that it may be too heavy for aerospace applications). The higher atomic weights also imply that the specific surface area (expressed in square meters per gram) is lower than it would be for less dense constituent materials. Thus, if compared on a surface area per volume of primary material, ACS would appear more like silica aerogel. This should not be an issue for industrial applications of these high porosity materials since weight is not a significant factor for most applications. The sintering tests confirmed that the material has excellent long term stability at high temperatures and so should be suitable for high lifetime applications.

Acknowledgements

This work was supported by the U.S. Department of Energy under contract no. DE-AC03-76SF00098 as part of the Office of Industrial Technologies-Industrial Materials of the Future Program. Particular mention of Charles Sorrell in his support of aerogel applications is gratefully acknowledged.

References

1. J.F. Poco, J.H. Satcher and L.W. Hrubesh. *J. Non-Cryst. Solids* **285** (2001), p. 57.

2. H. Hirashima, C. Kojima and H. Imai. *J. Sol–Gel Sci. Tech.* **8** (1997), p. 843.

3. Y. Mizushima and M. Hori. *J. Mater. Res.* **10** (1995), p. 1424.

4. H. Bozorgzadeh, E. Kemnitz, M. Nickkho-Amiry, T. Skapin and J.M. Winfield. *J. Fluorine Chem.* **110** (2001), p. 181.

5. M.K. Younes and A. Ghorbel. *Appl. Catal. A-Gen.* **197** (2000), p. 269.

6. J. Kirchnerova, D. Klvana and J. Chaouki. *Appl. Catal. A-Gen.* **196** (2000), p. 191.

7. M.K. Younes, A. Ghorbel and C. Naccache. *J. de Chim. Phys., Physico-Chimie Biol.* **94** (1997), p. 1993.

8. L. Le Bihan, F. Dumeignil, E. Payen and J. Grimblot. *J. Sol–Gel Sci. Technol.* **24** (2002), p. 113.

9. J. Walendziewski and M. Stolarski. *React. Kinet. Catal. Lett.* **71** (2000), p. 201. 10. A. Pierre, R. Begag and G. Pajonk. *J. Mater. Sci.* **34** (1999), p. 4937.

11. K. Tadanaga, T. Iwami, T. Minami and N. Tohge. *J. Ceram. Soc. Jpn.* **103** (1995), p. 582.

12. A.E. Gash, T.M. Tillotson, J.H. Satcher, L.W. Hrubesh and R.L. Simpson. *J. Non-Cryst. Solids* **285** (2001), p. 22

13. T. Skapin. *J. Non-Cryst. Solids* **285** (2001), p. 128.

14. B.E. Yoldas. *J. Mater. Sci.* **11** (1976), p. 465

15. T. Horiuchi, T. Osaki, T. Sugiyama, K. Suzuki and T. Mori. *J. Non-Cryst. Solids* **291** (2001), p. 187.

16. M.R. Ayers, A. A. White, X.Y. Song, and A. J. Hunt. *J. Non-Cryst. Solids* **291** (2003), p. 173.

17. P.H. Tewari, A.J. Hunt and K.D. Lofftus. *Mater. Lett.* **3** (1985), p. 363

18. S.Q. Zeng, A.J. Hunt, and R. Greif, "Theoretical Modeling of Carbon Content to Minimize the Heat Transfer in Silica Aerogel, "Journal of Non-Crystalline Solids, *186*, 271-277, 199

19. S.Q. Zeng, P.C. Stevens, A.J. Hunt, R. Greif, and D. Lee, "Thin Film Heater Thermal Conductivity Apparatus and Measurements of Thermal Conductivity of Silica Aerogel," International Journal of Heat and Mass Transfer, *39* , 2311-2317 1996.

20. D. Lee, P.C. Stevens, S.Q. Zeng and A.J. Hunt "Thermal Characterization of Carbon Opacified Silica Aerogels," J. Non-Crystalline Solids, *186*, 285-290, 1995.